

Molecular Dynamics Simulation of Ion Mobility. 2. Alkali Metal and Halide Ions Using the SPC/E Model for Water at 25 °C[†]

Song Hi Lee

Department of Chemistry, Kyungsoong University, Pusan 608-736, Korea

Jayendran C. Rasaiah*

Department of Chemistry, University of Maine, Orono, Maine 04469

Received: October 16, 1995; In Final Form: November 10, 1995[⊗]

We present results of computer simulations of the mobilities of the alkali metal ions (Li^+ , Na^+ , K^+ , Rb^+ , and Cs^+) and the halides (F^- , Cl^- , Br^- , and I^-) at 25 °C using the SPC/E model for water and ion–water parameters fitted to the binding energies of small clusters of ions. A simple truncation of the ion–water and water–water potentials was used, and the mobilities calculated from the mean square displacement and the velocity autocorrelation functions, respectively, were found to be in good agreement with each other. The calculations demonstrate, for the first time, cation and anion mobilities that fall on separate curves, as functions of ion size, with distinct maxima. This is in complete accord with experimental trends observed in water at 25 °C. The cation mobilities are also in better agreement with the measured values than the calculations done earlier (*J. Chem. Phys.* **1994**, *101*, 6964) using the TIP4P model. The mobilities of the halides calculated here for the SPC/E model are however slightly lower than the experimental results. The residence times of water in the hydration shells around an ion are found to decrease dramatically with its size. Stereoscopic pictures show that the structure of the solvent cage around an ion is qualitatively different for the larger ions, implicating both solvent dynamics and structure as important factors in explaining ion mobility in aqueous systems.

I. Introduction

The mobilities of ions in water¹ have been studied experimentally for over a century,² and they play an important role in solution chemistry, biochemistry, and some aspects of cell and membrane biology.³ They have also been investigated theoretically^{4–13} using continuum and discrete models for the solvent, but even the ion mobilities at infinite dilution are as yet incompletely understood. A fundamental problem that requires a detailed molecular explanation¹ is the observed maximum in the mobilities of the ions as a function of size and its weaker dependence on the sign of the ion charge. The latter observation immediately rules out simple dipolar or dielectric continuum solvent models that do not distinguish between the dynamical behavior of identical positive and negative ions of the same charge magnitude.

The use of molecular dynamics (MD) simulation methods to study ionic mobility has a relatively recent history that began with the work of Ciccotti and Jacucci¹⁴ and has continued through the efforts of many others.^{15–27} These studies have provided an important source of microscopic information about the subject, and there is now increasing interest in the dependence of ion mobility on the dynamical properties of the solvent apart from the expected dependence on the solvent dielectric constant and viscosity and the size and charge of the ions.

The explanation of the mobility of light ions like H^+ in water is a quantum mechanical problem that can be investigated by path integral methods together with ab initio calculations of the intermolecular interactions.^{28,29} Classical mechanics however is an adequate first approximation for the dynamics of the heavier alkali metal and halide ions in aqueous solution, but

for computer simulations to be useful, one must have reliable and consistent potential energy functions for the water–water and ion–water interactions. The other problems that remain with classical simulations are insufficient statistics for a single ion and, more seriously, an accurate but economical representation of the slowly decaying Coulombic interactions in an infinite system and the type of boundary conditions to be used.

In our previous work,²⁴ a series of MD simulations were performed on model cation–water systems at 25 °C, representing the behavior of Li^+ , Na^+ , K^+ , Rb^+ , and Cs^+ in an electric field of 1.0 V/nm and in its absence. The TIP4P model^{30a} was used for water, and TIPS potentials^{30b,30c} were adapted for the ion–water interactions together with the Steinhauser switching function,³¹ which smoothly reduces the interaction energy from its value at $r = R_L$ to zero at $r = R_U$ (R_L was usually chosen as $0.95R_U$ with $R_U \approx 9 \text{ \AA}$). The mobilities of the cations calculated directly from the drift velocity and the distance traveled by the ion were in good agreement with each other, and they were also in satisfactory agreement with those determined from the mean square displacement and the velocity autocorrelation function in the absence of the field. Remarkably, they all showed the same trends with ionic radii that are observed experimentally for the alkali metal cations, although the magnitudes were smaller than the experimental values in real water at 25 °C by almost a factor of 2. We also observed, in our simulations, that the water molecules in the first solvation shell around the small Li^+ ion are stuck to the ion and move with it as an entity for about 190 ps, while the waters in this shell around the Na^+ ion remain for 35 ps and those around the large cations remain for 8–11 ps before significant exchange with the surroundings occurs.

More recently there have been reports^{25–27} of spurious effects that the switching function has on ionic mobilities. It turns out that the Steinhauser switching function³¹ causes distortions of the velocity autocorrelation function that lead to ionic mobilities

[†] This paper is dedicated to Professor Harold L. Friedman on his retirement.

[⊗] Abstract published in *Advance ACS Abstracts*, December 15, 1995.

that may be too large, in extreme cases, by a factor of up to 5!²⁵ The effects also show up as unphysical behavior^{25,26} in the radial distribution and orientational correlation functions in the region of the switch off, which is about 9–10 Å away from the central ion in our calculations.²⁴ Indeed, signs of such unphysical behavior are just visible in Figures 6 and 7 of our previous work,²⁴ and the smaller magnitudes of the calculated mobilities in comparison to the experimental values could be partly attributed to the use of this switching function. However, the observed trends in the cation mobilities with ionic radii, which are qualitatively in accord with experiment, are less likely to be radically altered by truncation or a switch off function that affects the mobilities of ions of the same sign and charge to the same degree.

It has also been reported²⁶ that a simple truncation of the potential at a sufficiently large distance, when applied to simulations of just one ion, produced results that are very similar to the results in which Ewald sums or reaction field methods^{34–36} are used to include long-ranged Coulomb effects. However, such a scheme is not recommended in simulations with more than one ion, since the cutoff produces artificial correlations between ions.²⁶ We accordingly use the simple truncation scheme in this paper for our simulations of single ion mobility and leave the more elaborate and expensive computations using Ewald sums or reaction fields^{34–36} for a subsequent communication.

Our main objective, in this paper, is directed toward obtaining the first global view of ion mobilities at infinite dilution of alkali metal ions and the halides in water at 25 °C by computer simulation, using a more accurate and self consistent set of potential energy functions for the ion–water and water–water interactions. We report the results of MD simulations using the SPC/E potential³⁷ for water molecules and analogous ion–water potentials that have been fitted to the solvation energies of small ion–water clusters particularly by Dang and co-workers.^{38–43} Our results for the mobilities of the alkali metal ions are in closer accord with experiment, and our calculations for the halides agree qualitatively with the experimental observation that their mobilities lie on a separate curve as a function of the size with a maximum that is distinct from the maximum for the cations. The calculations presented here are, to our knowledge, the first to show that this characteristic experimental result can be replicated in computer simulations with currently available ion–water and water–water potentials. This opens the way to a detailed study of the underlying cause at a molecular level.

The paper is organized as follows. Section II contains a brief description of molecular models and MD simulation methods followed by section III, which presents the results of our simulations, and our conclusions are summarized in section IV.

II. Molecular Dynamics Simulations

In the present study, we have selected nine systems involving each of nine ions—fluoride, chloride, bromide, iodide, lithium, sodium, potassium, rubidium, or cesium ion—solvated in 215 water molecules at 298.15 K. Each simulation was carried out in the NVT ensemble, and the density was fixed at 0.997 g/cc, which corresponds to a cubic box length of 18.64 Å for the simulation. The usual periodic boundary condition in the *x*-, *y*-, and *z*-directions and the minimum image convention for pair potential were applied.

The SPC/E (extended simple point charge) model was adopted for the water molecule. It is a reparametrization of the simple point charge (SPC) model for water at 25 °C that improves the effective pair potential, leading to better values

TABLE 1: Halide–Water, Alkali Metal Cation–Water, and Water–Water Potential Parameters (SPC/E Model)^a

ion/water	σ_{io} (Å)	ϵ_{io} (kJ/mol)	charge (q)	ref
F ⁻	3.143	0.6998	-1	38
Cl ⁻	3.785	0.5216	-1	40
Br ⁻	3.896	0.4948	-1	44
I ⁻	4.168	0.5216	-1	39
Li ⁺	2.337	0.6700	+1	45
Na ⁺	2.876	0.5216	+1	43
K ⁺	3.250	0.5216	+1	43
Rb ⁺	3.348	0.5216	+1	43
Cs ⁺	3.526	0.5216	+1	41
O(H ₂ O)	3.169	0.6502	-0.8476	37
H(H ₂ O)			+0.4238	

^a In the SPC/E model for water, the charges on H are at 1.000 Å from the Lennard-Jones center at O. The negative charge is at the O site, and the HOH angle is 109.47°.

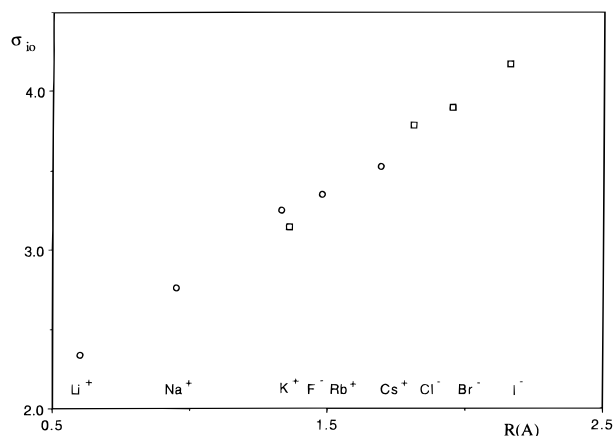


Figure 1. Ion–oxygen σ_{io} (Å) parameter as a function of the crystallographic radius R (Å) of the ion.

of the diffusion coefficient and a configurational energy which includes a self polarization energy correction.³⁷ The oxygen–oxygen radial distribution function is also somewhat improved although the first peak is shifted inward and is too high compared to both the experimental results and the calculated SPC values.

All nine ions were represented by a point charge having a Lennard-Jones (LJ) center on it. The potential parameters for ion–water and water–water interactions in this model, collected mostly from the work of Dang and collaborators,^{38–43} are listed in Table 1. There are two exceptions: the parameters for the Br⁻ ion are the ones fitted to the SPC model by Lybrand, Ghosh, and McCammon,⁴⁴ and the Li⁺ parameters are for the revised polarizability model (RPOL) of water developed by Dang.⁴⁵ Thus the parameters for Br⁻ may be slightly anomalous due to optimization with respect to the SPC rather than the SPC/E model. Likewise the parameters for Li⁺ are also not entirely consistent with the rest, since they were obtained for the revised polarizability (RPOL) model for water which, although similar to the SPC/E model, includes explicitly the atomic polarizabilities of the hydrogen and oxygen atoms in water. The polarizability of the Li⁺ in this model is relatively small (0.029 Å³) and is ignored implicitly in our study by using the RPOL σ_{io} and ϵ_{io} parameters for Li⁺ (Table 1) with the SPC/E parameters for water.

Apart from these two exceptions Table 1 provides a consistent set of water oxygen ion parameters fitted to gas phase binding energies of small ion–water clusters for the same SPC/E model for water. Figure 1 shows that the ion–water distance σ_{io} is linearly related to the crystallographic radius R but the well-depth (Figure 2) follows no such simple behavior.

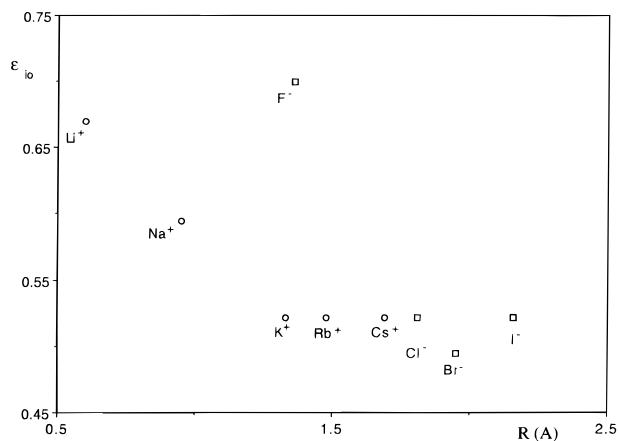


Figure 2. Ion–oxygen ϵ_{10} (kJ mol^{-1}) parameter as a function of the crystallographic radius R (\AA) of the ion.

A spherical cutoff ($R_c = 9.0 \text{ \AA}$) was employed for all the pair interactions. This is a simple truncation in which two molecules are considered as interacting if the distance between their centers is less than the cutoff radius R_c and the interaction is neglected if the distance is larger than R_c . This procedure introduces an artificial discontinuity in the pair potential at a distance $r = R_c$ from the central molecule or ion. In our previous study,¹¹ we employed the Steinhauser switching function¹⁸ instead, which smoothly reduces the interaction energy from its value at $r = R_L$ to zero at $r = R_U$ to avoid the discontinuity in the potential. This has been often used in the previous simulations^{7–9,11} in order to avoid the sudden warm up of the system, due to the energy discontinuity when the simple truncation is employed. Recent studies^{25,26} have reported that although the switching function stabilizes the system's temperature, it can cause other problems, as discussed in section I.

We used Gaussian isokinetics^{46–48} to keep the temperature of the system constant and the quaternion formulation⁴⁹ of the equations of rotational motion about the center of mass of the SPC/E water molecules. For the integration over time, we adapted Gear's fifth-order predictor–corrector algorithm⁵⁰ with a time step of 10^{-15} s (1 fs). Molecular dynamics (MD) runs of 100 000 time steps each were needed for the ion–water system to reach equilibrium. The equilibrium properties were then averaged over 10 blocks of 20 000 time steps (20 ps) for a total of 200 000 (200 ps). The configurations of molecules were stored every five time steps for further analysis.

III. Results and Discussion

In this section we present the results of our MD simulations at 298.15 K; the principal static and dynamic properties are considered separately.

A. Static Properties and Energetics. The average potential energies of ion–water and water–water are listed in Table 2, and the radial distribution functions for the ions and the O or H atoms of water molecules are shown in Figures 3–5. The potential energy for water includes a polarization correction³⁷ of 5.2 kJ per mol. Table 3 contains the positions and magnitudes of the maxima and minima of $g_{10}(r)$ in the first and second shells together with the corresponding values for the oxygen distribution functions $g_{00}(r)$ in pure water at 25 °C. The magnitude and position of the first peak in the chloride–oxygen (Cl^- -O) radial distribution functions (4.06 at $\sim 3.2 \text{ \AA}$) agree closely with the previous results⁵⁰ of the Cl^- -TIP4P water model, since the

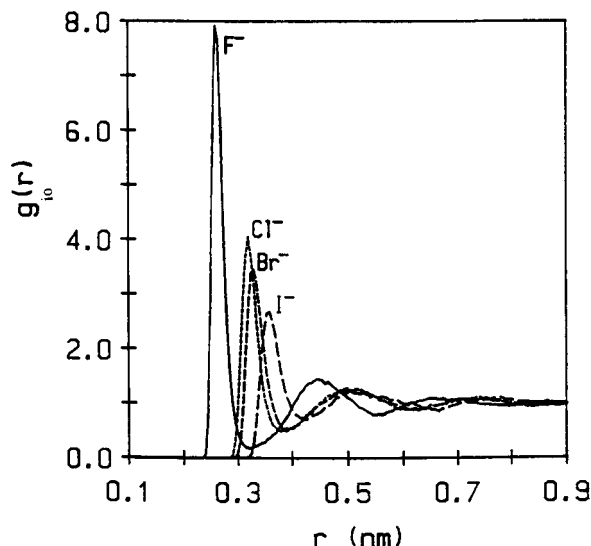


Figure 3. Radial distribution functions $g_{10}(r)$ of SPC/E water molecules as a function of the distance r_{10} between the anion (i) and the oxygen atom (o) of a water molecule.

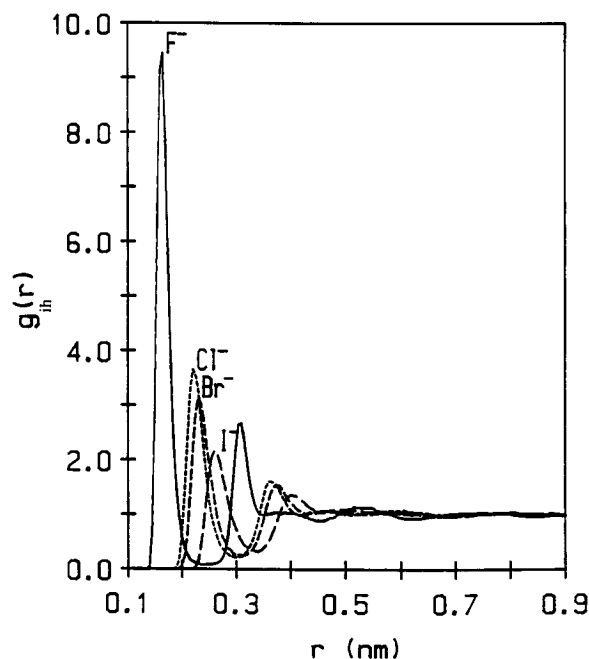


Figure 4. Radial distribution functions $g_{1h}(r)$ of SPC/E water molecules as a function of the distance r_{1h} between the anion (i) and the hydrogen atom (h) of a water molecule.

TABLE 2: Average Ion–Solvent, Solvent–Solvent Potential Energies and Diffusion Coefficients of Water Calculated from the MSD at 25 °C

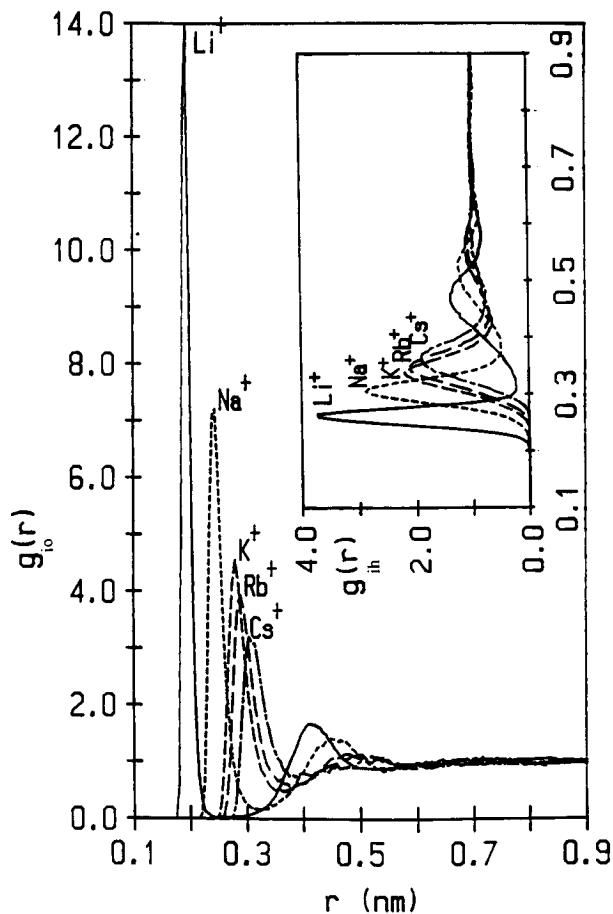
	U (kJ/mol)		D_w ($\times 10^{-5}$ cm ² /s) MSD
	ion–water	water–water	
F [−]	-840.4 ± 6.0	-39.5 ± 0.1	2.96 ± 0.11
Cl [−]	-575.6 ± 8.4	-40.0 ± 0.1	3.09 ± 0.15
Br [−]	-539.0 ± 2.8	-40.1 ± 0.1	2.90 ± 0.05
I [−]	-460.1 ± 5.4	-40.2 ± 0.1	2.84 ± 0.09
Li ⁺	-912.0 ± 6.5	-39.6 ± 0.2	3.19 ± 0.23
Na ⁺	-745.0 ± 3.7	-39.8 ± 0.1	3.03 ± 0.16
K ⁺	-606.5 ± 1.7	-40.1 ± 0.1	3.04 ± 0.10
Rb ⁺	-571.0 ± 1.7	-40.3 ± 0.1	2.96 ± 0.08
Cs ⁺	-534.4 ± 5.6	-40.5 ± 0.1	2.73 ± 0.06
H ₂ O		-41.4 ± 0.1	2.59 ± 0.08

LJ parameters are almost the same ($\sigma_{\text{ClO}} = 3.7835 \text{ \AA}$ and $\epsilon_{\text{ClO}} = 0.5216 \text{ kJ/mol}$ for SPC/E, and 3.7916 \AA and 0.5661 kJ/mol , respectively, for TIP4P). Calculations²⁷ for this system using

TABLE 3: Positions and Magnitudes at Maxima and Minima of Ion–Oxygen g_{io} and Oxygen–Oxygen g_{oo} Radial Distribution Functions at 25 °C

ion	first max		first min		second max		second min	
	r_{io} (Å)	g_{io}	r_{io} (Å)	g_{io}	r_{io} (Å)	g_{io}	r_{io} (Å)	g_{io}
F ⁻	2.60	7.92	3.20	0.17	4.45	1.45	5.50	0.79
Cl ⁻	3.20	4.06	3.80	0.49	5.00	1.28	6.05	0.89
Br ⁻	3.30	3.46	3.85	0.52	5.05	1.23	6.15	0.88
I ⁻	3.60	2.68	4.30	0.72	5.05	1.25	6.65	0.85
Li ⁺	1.95	14.00	2.65	0.02	4.10	1.69	5.25	0.89
Na ⁺	2.45	7.21	3.25	0.16	4.50	1.42	5.40	0.84
K ⁺	2.80	4.57	3.65	0.47	4.75	1.15	5.80	0.90
Rb ⁺	2.90	3.94	3.75	0.59	5.10	1.14	5.90	0.89
Cs ⁺	3.05	3.20	3.85	0.74	5.40	1.09	6.25	0.90

H ₂ O	r_{oo} (Å)		g_{oo}		r_{wo} (Å)		g_{oo}	
	r_{oo} (Å)	g_{oo}	r_{oo} (Å)	g_{oo}	r_{wo} (Å)	g_{oo}	r_{oo} (Å)	g_{oo}
H ₂ O	2.75	2.98	3.30	0.83	4.50	1.10	5.65	0.90

**Figure 5.** Radial distribution functions $g_{io}(r)$ of SPC/E water molecules as a function of the distance r_{io} between the cation (i) and the oxygen atom (o) of a water molecule. The inset shows the corresponding radial distribution functions $g_{ih}(r)$ as a function of the distance r_{ih} between the cation (i) and the hydrogen atom (h) of a water molecule.

Ewald sums and the TIP4P model showed that the $g_{ClO}(r)$ has its first peak at ~ 3.2 Å with a peak height of ~ 3.8 .

The heights of the first peaks in the bromide–oxygen (Br⁻O) and bromide–hydrogen (Br⁻H) radial distribution functions (3.46 Å at ~ 3.3 Å and 3.15 Å at ~ 2.3 Å) in our simulations are also in general accord with independent studies²⁵ of the bromide ion in SPC water which assume $\sigma_{BrO} = 4.103$ Å and $\epsilon_{BrO} = 0.4193$ kJ/mol.

When the radial distribution functions (Figure 5) for the cations and O atoms of water molecules in the present studies are compared with those of our previous study using the TIP4P water model,²⁴ the results are qualitatively similar except for the Li–O case. The large increase in the height and the decrease

TABLE 4: Average Coordination Number and Residence Times (ps) of Water Molecules in Hydration Shells of an Ion or Water Molecule at 25 °C^a

ion	hydration number	residence time (ps)
F ⁻	6.4 (18.2)	28.5 (10.9)
Cl ⁻	7.4 (24.7)	9.0 (9.0)
Br ⁻	7.2 (24.4)	9.5 (8.9)
I ⁻	8.1 (30.0)	7.7 (10.6)
Li ⁺	4.1 (16.1)	~ 400 (11.6)
Na ⁺	5.9 (17.5)	26.4 (9.8)
K ⁺	7.2 (21.2)	9.4 (9.6)
Rb ⁺	7.8 (21.0)	9.3 (8.5)
Cs ⁺	9.6 (21.3)	9.5 (9.3)
H ₂ O (SPC/E)	4.3 (16.9)	4.5 (8.3)

^a Numbers in parentheses are for the second hydration shell in column 2 (hydration number) and for the first and second shells in column 3 (the residence times).

in the Li–O distance of the first peak may be due to differences between the two water models—SPC/E and TIP4P—especially the positions of the point charge on the water molecule or excessively long equilibration times. Also, the average coordination number of water molecules around the Li⁺ ion shown in Table 4 is decreased in the SPC/E model from its value in the TIP4P model.

Table 4 displays average coordination numbers of water molecules in the first solvation shell alone and in the first and second solvation shells of the ions, calculated from our simulations. These numbers can be compared with previous results, which are 4.1,¹⁷ 5.8,^{19,45} 6.2,^{26,28} and 6.0⁵¹ for F⁻, 8.3,¹⁷ 7.2,^{19,27} 7.3,²⁶ 7.5⁰ and 6.9⁴⁰ for Cl⁻, 7.6²⁶ for Br⁻, 5.31⁹ and 6.0^{24,30c} for Li⁺, 6.0,^{17,19} 5.8,³⁸ and 6.6²⁴ for Na⁺, 6.3,¹⁷ 7.5,¹⁹ 7.9,²⁴ and 7.8 for Rb⁺,²⁴ and 9.6 for Cs⁺.²⁴ We discuss the dynamics of the solvation shells in the next section.

An examination of stereoscopic pictures of equilibrium configurations of water in the first solvation shell alone and the first and second solvation shells of F⁻, I⁻, Li⁺, and Cs⁺, respectively, shows that all the OH vectors of water molecules in the first shell around the F⁻ ion point toward the ion, while the directions of some of the OH vectors pointing toward the I⁻ ion are disturbed by hydrogen bonding to water molecules in the second solvation shell. Water molecules around the I⁻ ion are more loosely packed together than those around the F⁻ ion, and this appears to have a greater effect on the diffusive motion of I⁻ than F. Similar behavior of water dipoles is observed around the cations, but the water dipoles around the Cs⁺ ion are more disrupted than the dipole around the I⁻ ion.

B. Dynamic Properties. The diffusion coefficients (D), calculated from the mean square displacement (MSD) of the ions and from the velocity autocorrelation functions (VAC), are listed in Table 5. The ionic mobilities (u), determined from

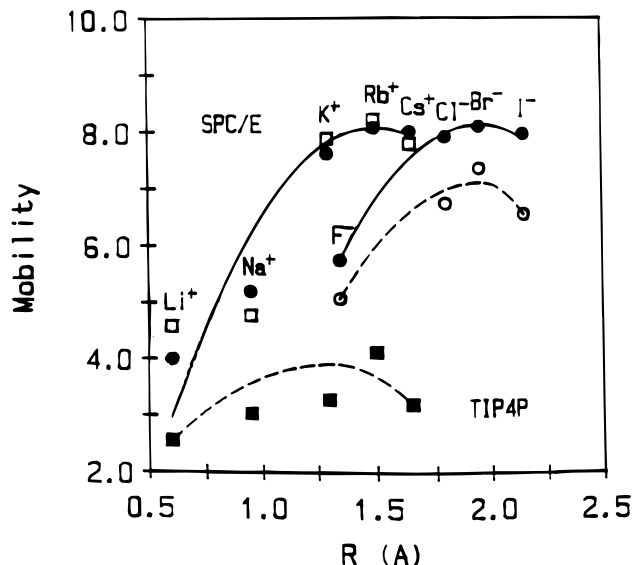


Figure 6. Ion mobilities in units of $10^{-4} \text{ cm}^2/(\text{V s})$ as a function of the crystallographic radius R (\AA) calculated from the mean square displacements of the anions (\circ) and the cations (\square), respectively, in SPC/E water. The corresponding mobilities for cations in TIP4P water²⁴ are shown as dark boxes (\blacksquare), and the experimental values are the points depicted as dark circles (\bullet).

TABLE 5: Diffusion Coefficient D and Mobility u of Halides and Alkali Metal Cations at Infinite Dilution in Water at 25 °C Calculated from the Mean Square Displacements and Velocity Autocorrelation Functions

ion	D ($\times 10^{-5} \text{ cm}^2/\text{s}$)		u ($\times 10^{-4} \text{ cm}^2/(\text{V s})$)	
	MSD	VAC	MSD	VAC
F^-	1.30 ± 0.42	1.29 ± 0.38	5.06 ± 1.63	5.02 ± 1.48
Cl^-	1.73 ± 0.42	1.71 ± 0.29	6.73 ± 1.63	6.65 ± 1.13
Br^-	1.89 ± 0.24	1.87 ± 0.22	7.35 ± 0.93	7.27 ± 0.86
I^-	1.68 ± 0.41	1.78 ± 0.40	6.54 ± 1.59	6.93 ± 1.55
Li^+	1.18 ± 0.09	1.27 ± 0.13	4.59 ± 0.35	4.79 ± 1.36
Na^+	1.22 ± 0.47	1.22 ± 0.45	4.75 ± 1.83	5.45 ± 1.75
K^+	2.02 ± 0.45	2.17 ± 0.42	7.86 ± 1.75	8.45 ± 1.63
Rb^+	2.11 ± 0.46	2.20 ± 0.47	8.21 ± 1.79	8.56 ± 1.83
Cs^+	2.00 ± 0.35	1.99 ± 0.39	7.78 ± 1.36	7.74 ± 1.52

these diffusion coefficients using the Einstein relation $u = Dq/kT$, are also listed in the same table. They are compared, in Figure 6, with the experimental results and with our previous simulations for the alkali metal cations using the TIP4P model for water. Table 2 also records the diffusion coefficients of water D_w in pure SPC/E water and in the ionic systems that were studied; they were calculated from the MSD of water molecules.

Figure 6 shows that the ionic mobilities of the anions are underestimated by about 20% in our simulations, while those of the cations are in better agreement with experiment. The experimental trends in the mobilities as a function of ionic radii are also observed in our simulations of univalent cations and anions with distinct maxima. The ionic mobilities of the cations obtained from our previous simulations using TIP4P water were clearly underestimated.

The residence time correlation function^{19,24} is defined by

$$R(r,t) = \frac{1}{N_r} \sum_{i=1}^{N_r} [\theta(r,0) \theta(r,t)] \quad (3.1)$$

where $\theta(r,t)$ is the Heaviside unit step function, which is 1 if a water molecule i is in a region r within the first coordination shell of the ion and 0 otherwise, and N_r is the average number

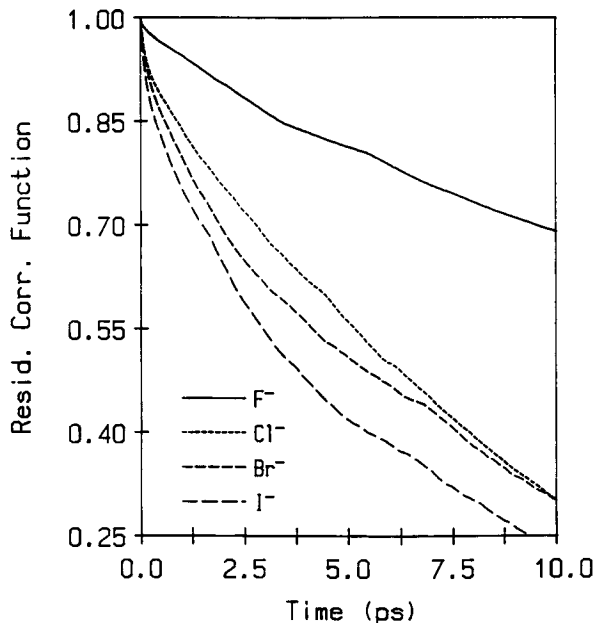


Figure 7. Residence time correlation function for the hydrated SPC/E water molecules in the first hydration shell of each anion.

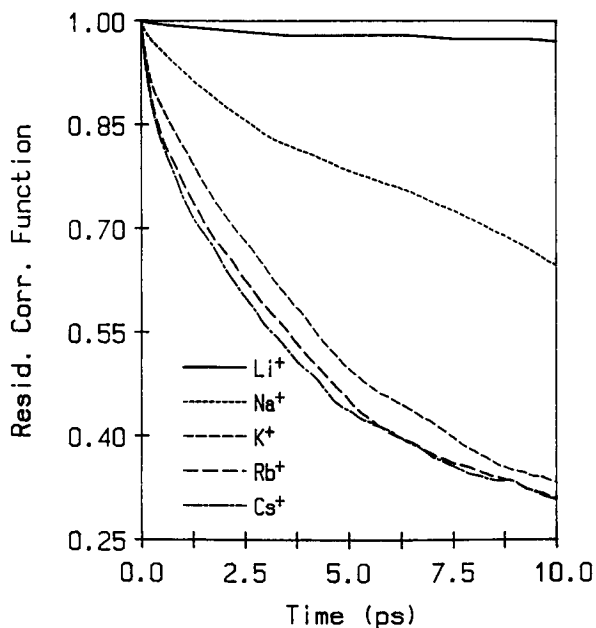


Figure 8. Residence time correlation function for the hydrated SPC/E water molecules in the first hydration shell of each cation.

of water molecules in this region r at $t = 0$. Figures 7 and 8 show the time dependence of $R(r,t)$ for water around the anions and cations, respectively, calculated in our simulations. The characteristic decay time, τ , is defined by the relation

$$\tau = \int_0^{\infty} \langle R(r,t) \rangle dt \quad (3.2)$$

but was obtained by fitting the time correlation function to an exponential decay $\langle R(r,t) \rangle \approx \exp(-t/\tau)$, which is useful particularly when τ is large.

The decay times, also listed in Table 4, show the average decay times of water in the first shell alone and also in the first and second shells. We note that these times decrease rapidly with increasing ion size and that the decay time for water in the first shell around Li^+ is even larger than what was found previously in the TIP4P model.

IV. Conclusions and Comments

Our calculations demonstrate, for the first time, that the unusual behavior of experimentally determined cation and anion mobilities at infinite dilution in aqueous systems at 25 °C can be reproduced in molecular dynamics simulations using the SPC/E model for water and simple pairwise additive ion–water potentials derived from the binding energies of ion–water clusters.^{38–43} This paves the way for a detailed study of the mechanism of ion transport and the influence of solvent structure and dynamics on the mobility of ions in aqueous solution.

Improvements to the model potentials and the computational techniques, especially by using Ewald sums or reaction fields to take account of the long-range forces, are in progress. We expect that the same trends will be observed in the mobilities as a function of ion size although the quantitative agreement with experiment for the cations may be slightly worse. Work in progress shows that Ewald sums have a greater effect on the negative ions than on the cations for the model considered, bringing the simulated mobilities for the anions closer to experiment. However, we caution that the use of Ewald sums or reaction fields with potentials fitted to the binding energies of small clusters of a solvated ion, that are by construction of limited extent and range, may not be always optimal or even completely consistent.

We have implicitly assumed, in our study, that the non-Newton trajectories of our Gaussian isokinetic simulations mimic the time evolution of a real system at constant temperature correctly to enable the diffusion coefficient to be calculated from the mean square displacement and the velocity autocorrelation function. This seems plausible but, as far as we know, has not been proved rigorously, although the question was raised some time ago.⁵³

The single most important requirement for observing in simulations subtle trends in the ion mobility as a function of ion size is the use of a consistent set of parameters for the ion–water and water interactions derived from the same model for water and parallel experimental data on ion–solvent energies of hydrated clusters of single ions.

Acknowledgment. This work was supported by Research Grant No. 911-0303-007-1 from the Korea Science and Engineering Foundation and by the Nondirected Research Fund of the Korea Research Foundation, 1992. S.H.L. thanks the Korea Institute of Sciences and Technology for access to the Cray-C90 super computer, and J.C.R. acknowledges the facilities provided by the Computer and Data Processing Services (CAPS) at the University of Maine. We thank Dr. Liem Dang for helpful communication on the potential parameters for ion–water interactions.

References and Notes

- (1) Frank, H. S. *Chemical Physics of Ionic Solutions*; John Wiley & Sons: New York, 1956; p 60.
- (2) (a) Robinson, R. A.; Stokes, R. H. *Electrolyte Solutions*, 2nd ed.; Butterworth: London, 1959. (b) Kay, R. L. In *Water, A Comprehensive Treatise*; Franks, F., Ed.; Plenum Press: New York, 1973; Vol. 3. (c) Harned, H. A.; Owen, B. B. *The Physical Chemistry of Electrolyte Solutions*; American Chemical Society Monograph; Reinhold Publishing Corporation: 1950.
- (3) (a) Rioux, B.; Karplus, M. *Annu. Rev. Biophys. Biomol. Struct.* **1994**, *23*, 731. (b) Goodfellow, J. M., Ed. *Computer Modeling in Molecular Biology*; VCH Publishers; New York, 1995. (c) Jordon, P. C. *Biophys. J.* **1990**, *58*, 1133.
- (4) Born, M. Z. *Phys.* **1920**, *1*, 221.
- (5) Fuoss, R. M. *Proc. Natl. Acad. Sci. U.S.A.* **1959**, *45*, 807.
- (6) Boyd, R. H. *J. Chem. Phys.* **1961**, *35*, 1281.
- (7) Zwanzig, R. *J. Chem. Phys.* **1963**, *38*, 1603; **1970**, *52*, 3625.
- (8) Hubbard, J.; Onsager, L. *J. Chem. Phys.* **1977**, *67*, 4850.
- (9) Hubbard, J. *J. Chem. Phys.* **1978**, *68*, 1649.
- (10) (a) Hubbard, J.; Kayser, R. F. *J. Chem. Phys.* **1981**, *74*, 3535. (b) Hubbard, J.; Kayser, R. F. *J. Chem. Phys.* **1982**, *76*, 3377.
- (11) (a) Wolynes, P. G. *J. Chem. Phys.* **1978**, *68*, 473. (b) Colonomos, P.; Wolynes, P. G. *J. Chem. Phys.* **1979**, *71*, 2644.
- (12) (a) Wolynes, P. *Annu. Rev. Phys. Chem.* **1980**, *31*, 345. (b) Hubbard, J.; Wolynes, P. Theories of Solvated Ion Dynamics. In *The Chemical Physics of Ion Solvation*; Dogonadze, R. R., Kalman, E., Kornyshev, A. A., Ulstrup, J., Eds.; Elsevier: Amsterdam, 1985; Part C, Chapter 1. (c) Hubbard, J. Non-Equilibrium Theories of Electrolyte Solutions. In *The Physics and Chemistry of Aqueous Ionic Solutions*; Bellissent-Funel, M. C., Neilson, G. W., Eds.; D. Reidel Publishing Company: Dordrecht, 1987.
- (13) Biswas, R.; Roy, S.; Bagchi, B. *Phys. Rev. Lett.* **1995**, *75*, 1098.
- (14) Ciccotti, G.; Jacucci, G. *Phys. Rev. Lett.* **1975**, *35*, 789.
- (15) Gosling, E. M.; Singer, K. *Chem. Phys. Lett.* **1976**, *39*, 361.
- (16) Pollock, E. L.; Alder, B. J. *Phys. Rev. Lett.* **1978**, *41*, 903.
- (17) Mezei, M.; Beveridge, D. L. *J. Chem. Phys.* **1981**, *74*, 6902.
- (18) Nguyen, H. L.; Adelman, S. A. *J. Chem. Phys.* **1984**, *81*, 4564.
- (19) Impey, R. W.; Madden, P. A.; McDonald, I. R. *J. Phys. Chem.* **1983**, *87*, 5071.
- (20) Wilson, M. A.; Pohorille, A.; Pratt, L. R. *J. Chem. Phys.* **1985**, *83*, 5382.
- (21) Berkowitz, M.; Wan, W. *J. Chem. Phys.* **1987**, *86*, 376.
- (22) Reddy, M. R.; Berkowitz, M. *J. Chem. Phys.* **1988**, *88*, 7104.
- (23) Rose, D. A.; Benjamin, I. *J. Chem. Phys.* **1993**, *98*, 2283.
- (24) Lee, S. H.; Rasaiah, J. C. *J. Chem. Phys.* **1994**, *101*, 6964.
- (25) del Buono, G.; Cohen, S. T. S.; Rossky, P. J. *J. Mol. Liq.* **1994**, *60*, 221.
- (26) Perera, L.; Essman, U.; Berkowitz, M. L. *J. Chem. Phys.* **1995**, *102*, 450.
- (27) Roberts, J. E.; Schnitker, J. *J. Phys. Chem.* **1995**, *99*, 1322. These authors also examined the room temperature properties of aqueous solutions of SPC,³² TIP4P,³⁰ and MCY³³ models for water using either a potential cutoff or Ewald summation.³⁴ Both pure water and dilute solutions of Cl⁻ and Fe²⁺ were investigated. They found not only solvent–solvent orientational correlations but also ion–solvent energies, ion-induced solvent reorganization energies, and ionic diffusion coefficients.
- (28) Carr, R.; Paraniello, M. *Phys. Rev. Lett.* **1985**, *55*, 2471.
- (29) Voth, G. A. *J. Phys. Chem.* **1991**, *95*, 10425.
- (30) (a) Jorgensen, W. L.; Madura, J.; Impey, W. R. W.; Klein, M. L. *J. Chem. Phys.* **1983**, *79*, 926. (b) Chandrasekhar, J.; Spellmeyer, D.; Jorgensen, W. L. *J. Am. Chem. Soc.* **1984**, *106*, 903. Jorgensen, W. L. *J. Chem. Phys.* **1982**, *77*, 4156.
- (31) Steinhäuser, O. *Mol. Phys.* **1982**, *43*, 335.
- (32) Berendsen, H. J. C.; Postma, J. P. M.; Van Gunsteren, W. F.; Hermans, J. In *Intermolecular Forces*; Pullman, B., Ed.; Reidel: Dordrecht, 1981.
- (33) Matsuoka, O.; Clementi, E.; Yoshimine, M. *J. Chem. Phys.* **1976**, *64*, 1351.
- (34) De Leeuw, S. W.; Perram, J. W.; Smith, E. R. *Proc. R. Soc. London.* **1980**, *A373*, 27.
- (35) Barker, J. A.; Watts, R. O. *Mol. Phys.* **1973**, *26*, 789.
- (36) Adams, D. J.; Adams, E. M.; Hills, G. *J. Mol. Phys.* **1979**, *38*, 387.
- (37) Berendsen, H. J. C.; Grigera, J. R.; Straatsma, T. P. *J. Phys. Chem.* **1987**, *91*, 6269.
- (38) Dang, L. X. *Chem. Phys. Lett.* **1992**, *200*, 21.
- (39) Dang, L. X.; Garrett, B. C. *J. Chem. Phys.* **1993**, *99*, 2972.
- (40) Smith, D. E.; Dang, L. X. *J. Chem. Phys.* **1994**, *100*, 3757.
- (41) Dang, L. X. *Chem. Phys. Lett.* **1994**, *227*, 211.
- (42) Dang, L. X.; Kollman, P. A. *J. Phys. Chem.* **1995**, *99*, 55.
- (43) Dang, L. X. *J. Am. Chem. Soc.* **1995**, *117*, 6954.
- (44) Lybrand, T. P.; Ghosh, I.; McCammon, J. A. *J. Am. Chem. Soc.* **1985**, *107*, 7793.
- (45) Dang, L. X. *J. Chem. Phys.* **1992**, *96*, 6970.
- (46) Gauss, K. F.; Reine, J. *Angew. Math.* **1829**, *IV*, 232.
- (47) Hoover, W. G.; Ladd, A. J. C.; Moran, B. *Phys. Rev. Lett.* **1982**, *48*, 1818.
- (48) Evans, D. J. *J. Chem. Phys.* **1983**, *78*, 3297.
- (49) (a) Evans, D. J. *Mol. Phys.* **1977**, *34*, 317. (b) Evans, D. J.; Murad, S. *Mol. Phys.* **1977**, *34*, 327.
- (50) Gear, W. C. *Numerical Initial Value Problems in Ordinary Differential Equations*; McGraw-Hill: New York, 1965.
- (51) Madura, J. F.; Pettitt, B. M. *Chem. Phys. Lett.* **1992**, *96*, 6970.
- (52) Narten, A. H. *J. Phys. Chem.* **1970**, *74*, 765.
- (53) Andersen, H. C. *J. Chem. Phys.* **1980**, *72*, 2384.